REPORT DOCUMENTATION PAGE

Form Approved
OMB No. 074-0188

Public reporting burden for this collection of information is estimated to average 1 hour per response, including the time for reviewing instructions, searching existing data sources, gathering and maintaining the data needed, and completing and reviewing this collection of information. Send comments regarding this burden estimate or any other aspect of this collection of information, including suggestions for reducing this burden to Washington Headquarters Services, Directorate for Information Operations and Reports, 1215 Jefferson Davis Highway, Suite 1204, Arlington, VA 22202-4302, and to the Office of Management and Budget, Paperwork Reduction Project (0704-0188), Washington, DC 20503

1. AGENCY USE ONLY (Leave blank)	2. REPORT DATE	3. REPORT TYPE AND DATES COVERED
	30 September 1993	Interim Report, 1993

4. TITLE AND SUBTITLE
Fluid-Modeling Studies of Convective Dispersion Processes

5. FUNDING NUMBERS
Cooperative Agreement No. CR821211

6. AUTHOR(S)
J.C. Wyngaard, Mark Piper and W.H. Snyder

7. PERFORMING ORGANIZATION NAME(S) AND ADDRESS(ES)

Department of Meteorology
The Pennsylvania State University

U.S. EPA
Research Triangle Park, NC 27711

8. PERFORMING ORGANIZATION REPORT NUMBER
N/A

9. SPONSORING / MONITORING AGENCY NAME(S) AND ADDRESS(ES)

SERDP
901 North Stuart St. Suite 303
Arlington, VA 22203

10. SPONSORING / MONITORING AGENCY REPORT NUMBER
N/A

11. SUPPLEMENTARY NOTES
Performed under Cooperative Agreement No. CR821211. This work was supported in part by SERDP. The United States Government has a royalty-free license throughout the world in all copyrightable material contained herein. All other rights are reserved by the copyright owner.

12a. DISTRIBUTION / AVAILABILITY STATEMENT
Approved for public release: distribution is unlimited

12b. DISTRIBUTION CODE
A

13. ABSTRACT ***(Maximum 200 Words)***

These experiments are part of a project whose objectives are to improve our understanding of diffusion in convective turbulence and to develop better models of this diffusion for a wide range of applications. Toward those ends, two diffusion problems are being studied in the Fluid modeling Facility (FMF) convection tank. The first concerns "transport asymmetry," the difference in the diffusion properties of scalars introduced at the bottom and top of convective boundary layers. The second area of study, the diffusion of highly buoyant plumes in the convective boundary layer, will be carried out under subcontract by Dr. J.C. Weil of CIRES at the University of Colorado.

19980817 148

14. SUBJECT TERMS	15. NUMBER OF PAGES
diffusion, convective dispersion, FMF, SERDP	19
	16. PRICE CODE: N/A

17. SECURITY CLASSIFICATION OF REPORT	18. SECURITY CLASSIFICATION OF THIS PAGE	19. SECURITY CLASSIFICATION OF ABSTRACT	20. LIMITATION OF ABSTRACT
unclass	unclass	unclass	UL

DTIC QUALITY INSPECTED 1

Interim Report

FLUID-MODELING STUDIES OF CONVECTIVE DISPERSION PROCESSES

J.C. Wyngaard and Mark Piper

Department of Meteorology
The Pennsylvania State University

Cooperative Agreement No. CR821211
Dr. W. H. Snyder, Project Officer
U.S. Environmental Protection Agency
Research Triangle Park, NC 27711

Funds for this cooperative agreement originated with the
Strategic Environmental Research and
Development Program (SERDP).

September 30, 1993

1. Introduction

This is a first report on diffusion experiments done in summer, 1993, at the EPA Fluid Modeling Facility (FMF) by Mark Piper with the generous guidance and assistance of their staff, including FMF director Bill Snyder and FMF scientist Bob Lawson.

These experiments are part of a project whose objectives are to improve our understanding of diffusion in convective turbulence and to develop better models of this diffusion for a wide range of applications. Toward those ends, two diffusion problems are being studied in the FMF convection tank. The first concerns "transport asymmetry", the difference in the diffusion properties of scalars introduced at the bottom and top of convective boundary layers. The second area of study, the diffusion of highly buoyant plumes in the convective boundary layer, will be carried out under subcontract by Dr. J. C. Weil of CIRES at the University of Colorado.

2. Theory of Top-Down, Bottom-Up Diffusion

During the 1980s the numerical technique called large-eddy simulation (LES) predicted striking differences between the "top-down" and "bottom-up" vertical diffusion from very large area sources within the convective boundary layer (CBL). Top-down diffusion is defined as that process in which the vertical turbulent flux of the scalar is zero at the surface and maximum at the mixed-layer top; in bottom-up diffusion the flux is zero at the top and maximum at the surface. For example, ozone introduced into the boundary layer by turbulent entrainment of the overlying atmosphere undergoes top-down diffusion. The bottom-up process—a scalar flux at the surface but not at the mixed-layer top—probably does not exist in isolation from the top-down one. This is because the entrainment process in conjunction with the change in the scalar concentration across the inversion "reflects" the bottom-up diffusion, generating a flux at the top as well. For example, solar heating generates a positive temperature flux at the surface, but the turbulent entrainment of the capping inversion brings down warmer air and, hence, generates a negative temperature flux at the mixed-layer top. Thus, a heated surface drives a combination of bottom-up and top-down diffusion of temperature, and an evaporating surface drives a combination of bottom-up and top-down diffusion of water vapor.

It is the linearity of the scalar diffusion process that makes the top-down, bottom-up concept a useful one. To illustrate, let us represent a scalar field $\tilde{c}$ in the CBL as $\tilde{c} = C + c$, the sum of ensemble-mean and fluctuating parts. One can decompose each of

$\tilde{C} = C + c$

these, in turn, into top-down and bottom-up components:

$$C = C_t + C_b; \qquad c = c_t + c_b. \tag{1}$$

The mean gradient and turbulent flux are thus the sum of top-down and bottom-up components:

$$\frac{\partial C}{\partial z} = \frac{\partial C_t}{\partial z} + \frac{\partial C_b}{\partial z}; \qquad \overline{cw} = \overline{c_t w} + \overline{c_b w}. \tag{2}$$

Wyngaard and Brost (1984) and Moeng and Wyngaard (1984) isolated the statistical properties of top-down and bottom-up diffusion from LES data. They found that the top-down eddy diffusivity

$$K_t = \frac{-\overline{c_t w}}{\partial C_t / \partial z} \tag{3}$$

is well-behaved, having a maximum magnitude of about $0.1 w_* z_i$ in midlayer. Here w_* is the convective velocity scale $(\beta Q_0 z_i)^{1/3}$, where β is the Boussinesq buoyancy parameter, Q_0 is the surface temperature flux, and z_i is the boundary-layer depth. The bottom-up diffusivity is everywhere larger in magnitude and has a midlayer singularity. This means that the well-documented failure of eddy diffusivity closure for scalars in the convective boundary layer (e.g., Deardorff, 1966) is confined to the bottom-up process.

Transport asymmetry has yet to be confirmed through direct observations in the atmosphere. It appears that a specially designed field program, with scatter minimized through optimally chosen scalars and long flight legs, is required to test the LES results in the atmosphere. One of our objectives is to test the hypothesis first in the laboratory.

3. Operation of the FMF Convection Tank

Fluid modeling allows one to simulate certain geophysical flows in the laboratory without precisely matching the values of all dimensionless parameters (Snyder, 1981). Deardorff and Willis began a long series of studies in a laboratory convection tank 1 m on a side, using water as the fluid, in the late 1960s; they soon perceived it as a model of the unstable planetary boundary layer (Willis and Deardorff, 1974). Research findings from this tank continued for nearly two decades (Deardorff and Willis, 1985). Their early diffusion studies, particularly after they were corroborated through LES, revolutionized the way we perceive convective plume dispersion (Lamb, 1982). These laboratory experiments have provided much of the present basis for short range atmospheric dispersion modeling under convective conditions (Weil, 1988).

The original Deardorff-Willis convection tank is now located in the Fluid Modeling Facility of the Atmospheric Research and Exposure Assessment Laboratory. The tank

sidewalls are constructed of 1.9 cm thick plexiglass, and the bottom is a 1.27 cm thick anodized aluminum plate. The horizontal inside dimensions of the tank are 122 cm × 124 cm; the depth is 45 cm. In the experiments done in the summer of 1993 we filled the tank to 35 cm depth with filtered, deaerated water. To minimize heat loss, 5 cm slabs of styrofoam are attached to the sidewalls of the tank and smaller pieces of 2 cm styrofoam are floated on the water free surface. To heat the lower surface of the tank, 144 electric heaters are affixed to the underside of the aluminum plate at the tank bottom. They are constructed of a metal foil insulated with rubber and coated with a pressure-sensitive adhesive on one side. Up to 6 kW total power can be dissipated through these heaters.

To simulate the inversion layer that lies above the daytime CBL, a stably stratified temperature profile was formed by passing a grid of heating wires through the upper 20 cm of water in the tank. The heating grid consists of four 102 m-long circuits of 2 mm teflon-coated wire, each circuit having a computed resistance of 19 ohms. A current of 2.9 amps was applied to the wires, giving a total power output of over 600 W.

In our experiments we heated the water between 15 and 35 cm to create an inversion of strength 0.5 C per cm. The depth of this stratified layer satisfies the criterion set by Deardorff and Willis (1985) that the aspect ratio of tank sidewall separation to layer depth be at least 5:1. We used two scalars, temperature and food dye, in our diffusion experiments.

Measurements of temperature diffusion

We measured horizontally averaged mean temperature with a resistance-wire grid formed by stringing 33 meters of 0.762 mm teflon-coated alumel wire across an aluminum frame. The grid frame was constructed from 1" x 1/8" aluminum strips and measures 120 cm on a side. We obtained vertical profiles of mean temperature by traversing the grid vertically through the tank at an average speed of 0.64 cm s^{-1}. A potentiometer marked the vertical position of the grid in the tank. The grid position in centimeters was interpolated from a two-point calibration table.

We used the voltage deflection across a Wheatstone bridge to measure the RTD grid wire resistance, which varies approximately linearly with temperature. A calibration table was compiled by measuring the bridge output voltage against a thermistor reading; temperature was then interpolated from this calibration table. A 10 Hz lowpass filter was used to remove noise from the output voltage signal.

A nominal value of 3 kW of power was dissipated through the heaters at the lower

surface of the tank. This rate of surface heating provides a turbulent Reynolds number based on layer depth z_i and velocity scale w_* of at least 1000.

During a data retrieval run, output voltage was sampled continuously at 56 Hz. A 14-point block average was immediately applied to the raw data, giving an effective sampling frequency of 4 Hz. Data retrieval runs varied in length from 10 to 50 min. Elapsed time, grid position, bridge voltage and temperature data were written to a ASCII file at a rate of 4 records per second.

Measurements of dye diffusion

We introduced the top-down scalar, food dye, as follows. The tank was initially filled to a depth of 32 cm with filtered, deaerated water and allowed to cool to nearly 21 C. We mixed 400 ml of dye with water for a nominal 45 liters of solution. This solution was kept at 40 C. To induce thorough mixing, the dye solution was introduced into the tank at a point slightly below the water free surface at an average flow rate of 25 ml s^{-1}. While the dye was being injected into the tank, the stratification system was also in operation, aiding in the mixing of the dye solution.

After the solution was completely siphoned into the tank, the dye layer extended from 15 cm to 35 cm, coinciding with the layer of stable temperature stratification in the tank. A small amount of dye tended to leak through the stable inversion layer; being negatively buoyant, it dropped to the surface of the tank. These dye streamers were quickly mixed and diluted shortly after the surface heating of the tank was initiated.

We sampled dye concentration by siphoning fluid through plastic tubing at 16 discrete levels at five locations in the convection tank. The fluid was collected in test tubes and analyzed with a photocolorimeter. The measured transmissivity of a light beam through the sampled fluid was compared against a calibration table of measured standards. This system is appealing because of its simplicity and because the sampling rakes fit between the RTD grid wires, allowing temperature and dye concentration to be sampled simultaneously.

4. Top-down, Bottom-up Diffusion—Preliminary Results

As we discussed, a scalar introduced at the surface undergoes both bottom-up and top-down diffusion, the latter being induced by the entrainment process in the capping inversion that marks the top of the convective layer. For that reason there seems to be no way to produce "pure" bottom up diffusion experimentally. Because the bottom sur-

face can be inpenetrable to some scalars (e.g., density of a diffusing constituent) "pure" top-down diffusion experiments can be done, however. In principle, using two different scalars, either simultaneously in one flow or sequentially in two statistically identical flows, allows one to deduce the mean transport properties of the top-down and bottom-up processes.

The mean temperature $T(z,t)$ in the convecting fluid layer evolves according to

$$\frac{\partial T}{\partial t} + \frac{\partial \overline{\theta w}}{\partial z} = 0. \tag{4}$$

Figure 1 shows the measured mean temperature versus height and time. From these data we calculated the vertical profiles of $\partial T/\partial t$ shown in Figure 2. From (4) this gives the divergence of the turbulent temperature flux. Integrating this flux divergence over z yields, from (4) and the lower boundary condition,

$$\overline{\theta w}(z) = \overline{\theta w}_0 - \int_0^z \frac{\partial T}{\partial t} dz' \simeq (1 - z/z_i)\, \overline{\theta w}_0 + (z/z_i)\, \overline{\theta w}_1, \tag{5}$$

since the profile is known to be essentially linear over the mixed layer. Since temperature undergoes both top-down and bottom-up diffusion, both the surface flux $\overline{w\theta}_0$ and the top flux $\overline{w\theta}_1$ are nonzero.

In principle the surface flux $\overline{\theta w}_0 = Q_0$ is known from the thermal energy balance for the lower plate of the convection tank, so the top flux $\overline{\theta w}_1$ can be found from (5). For reasons that are not yet clear, we found that this gave unrealistic flux profiles near the fluid layer top. Instead, we allowed the surface flux to be determined by (5) under the condition that the flux in the undisturbed flow deep in the inversion layer was zero. This gave the flux profiles in Figure 3. The height where the flux reaches its negative naximum is taken as z_i; it is indicated on each of the profiles in Figure 3.

Figure 4 shows on an expanded temperature scale a typical temperature record from the traversing probe. Since this record is from a moving probe, time varies with position along the profile. Converting this record to a single time yields the temperature profile in Figure 5. The noise level in this profile is encouragingly low. The resulting vertical gradient of temperature, scaled with z_i and the surface temperature scale $T_* = Q_0/w_*$, is shown in Figure 6. Also plotted there is a profile from large-eddy simulation of a convective boundary layer. The agreement is good except near the surface. We are currently investigating the reasons for the discrepancy there.

The mean concentration C_t of the food dye, entrained from the capping inversion

layer by convective eddies in the growing convective layer below, evolves as

$$\frac{\partial C_t}{\partial t} + \frac{\partial \overline{c_t w}}{\partial z} = 0. \tag{6}$$

LES experiments (Moeng and Wyngaard, 1984) indicate that during this process the scalar flux profile is nearly linear, so that

$$\overline{c_t w}(z) = \left(\frac{z}{z_i}\right) \overline{c_t w}(z_i) = \left(\frac{z}{z_i}\right) \overline{c_t w}_1, \tag{7}$$

and the top flux $\overline{c_t w}_1$ does not depend significantly on time. Thus, the mean gradient is quasi-steady,

$$\frac{\partial}{\partial t}\frac{\partial C_t}{\partial z} \simeq 0. \tag{8}$$

Figure 7 shows the measured mean concentration $C_t(z,t)$ at 16 heights z and five times t. The calculated time derivative $\partial C_t/\partial t$ is shown in Figure 8. The deduced top-down flux divergence is

$$\frac{\partial \overline{c_t w}}{\partial z} = -\frac{\partial C_t}{\partial t}, \tag{9}$$

and since by definition $\overline{c_t w}(0) = 0$, we can integrate this to get

$$\overline{c_t w}(z) = (z/z_i)\, \overline{c_t w}_1 = -\int_0^z \frac{\partial C_t}{\partial t} dz' = -z\frac{\partial C_t}{\partial t}. \tag{10}$$

The resulting flux profiles at the five times are shown in Figure 9.

Figure 10 shows the measured vertical gradient of mean dye concentration nondimensionalized with z_i and the concentration scale $c_* = \overline{c_t w}_1/w_*$. Since the dye diffusion is a top-down process, this nondimensionalized dye gradient is precisely the top-down gradient function g_t:

$$g_t(z/z_i) = -\frac{\partial C_t}{\partial z}\frac{z_i w_*}{\overline{c_t w}_1}. \tag{11}$$

The LES result for g_t (Moeng and Wyngaard, 1984) is shown in Figure 10 along with the dye data. The agreement is fairly good.

We estimated the bottom-up gradient function as follows. By the linearity of diffusion and the similarity hypothesis we have

$$\frac{\partial T}{\partial z} = \frac{\partial T_b}{\partial z} + \frac{\partial T_t}{\partial z} = -\frac{\overline{\theta w}_0}{w_* z_i} g_b - \frac{\overline{\theta w}_1}{w_* z_i} g_t. \tag{12}$$

Having the top-down gradient function g_t from the food-dye results, we used this equation to infer the bottom-up function g_b from the temperature data:

$$g_b = -\frac{w_* z_i}{\overline{\theta w}_0}\left(\frac{\partial T}{\partial z} + \frac{\overline{\theta w}_1}{w_* z_i} g_t\right). \tag{13}$$

Figure 11 shows the resulting g_b estimates and the corresponding LES results. The agreement is somewhat poorer that for g_t, Figure 10, principally because of the systematically low measured gradient values near the surface. Nonetheless, the LES results of transport asymmetry—that g_t at z/z_i is systematically larger than g_b at $(1 - z/z_i)$, so that the bottom up diffusivity K_b exceeds the top-down one K_t—is reproduced by the tank experiments.

5. References

Deardorff, J.W., 1966: The counter-gradient heat flux in the atmosphere and in the laboratory. *J. Atmos. Sci.*, **23**, 503–506.

Deardorff, J.W., and G.E. Willis, 1985: Further results from a laboratory model of the convective boundary layer. *Boundary-Layer Meteorol.*, **32**, 205–236.

Lamb, R.G., 1982: Diffusion in the convective boundary layer. *Atmospheric Turbulence and Air Pollution Modelling*, F.T.M. Nieuwstadt and H. van Dop, Eds., Reidel, Dordrecht, 159–229.

Moeng, C.-H., and J.C. Wyngaard, 1984: Statistics of conservative scalars in the convective boundary layer. *J. Atmos. Sci.*, **41**, 3161–3169.

Snyder, W.H., 1981: *Guideline for Fluid Modeling of Atmospheric Diffusion.* Report number EPA-600/8-81-009, Environmental Protection Agency, Research Triangle Park, NC. 200 pp.

Weil, J.C., 1988: Dispersion in the convective boundary layer. *Lectures on Air Pollution Modeling*, A. Venkatram and J.C. Wyngaard, Eds., Amer. Meteor. Soc., Boston, 167–227.

Willis, G.E., and J.W. Deardorff, 1974: A laboratory model of the unstable planetary boundary layer. *J. Atmos. Sci.*, **31**, 1297–1307.

Wyngaard, J.C., and R.A. Brost, 1984: Top-down and bottom-up diffusion of a scalar in the convective boundary layer. *J. Atmos. Sci.*, **41**, 102–112.

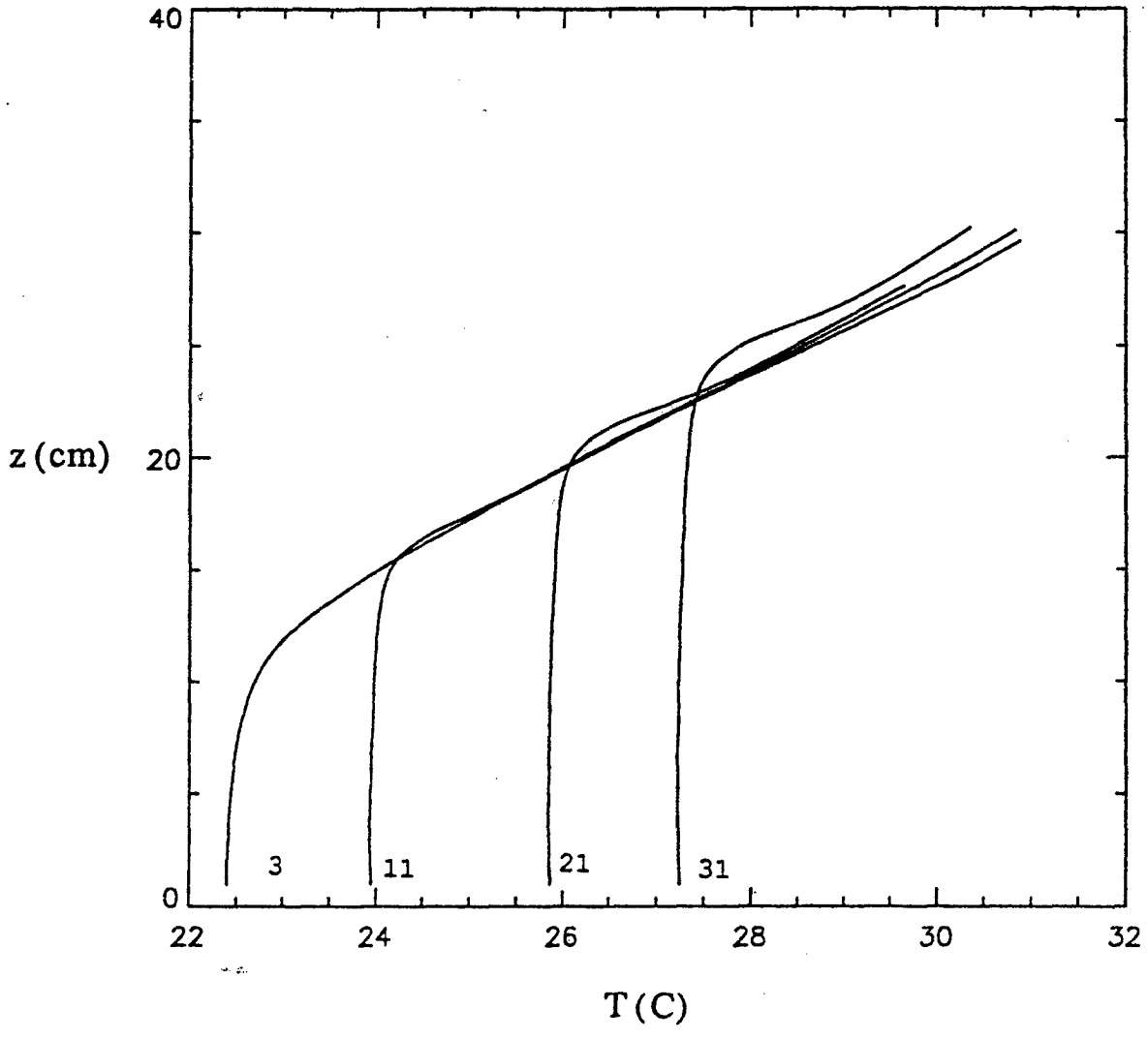

Figure 1. Mean temperature as a function of height and time for four traverses. Time increases with height along a given trace and with traverse number. Traverse 3 was taken before heating started.

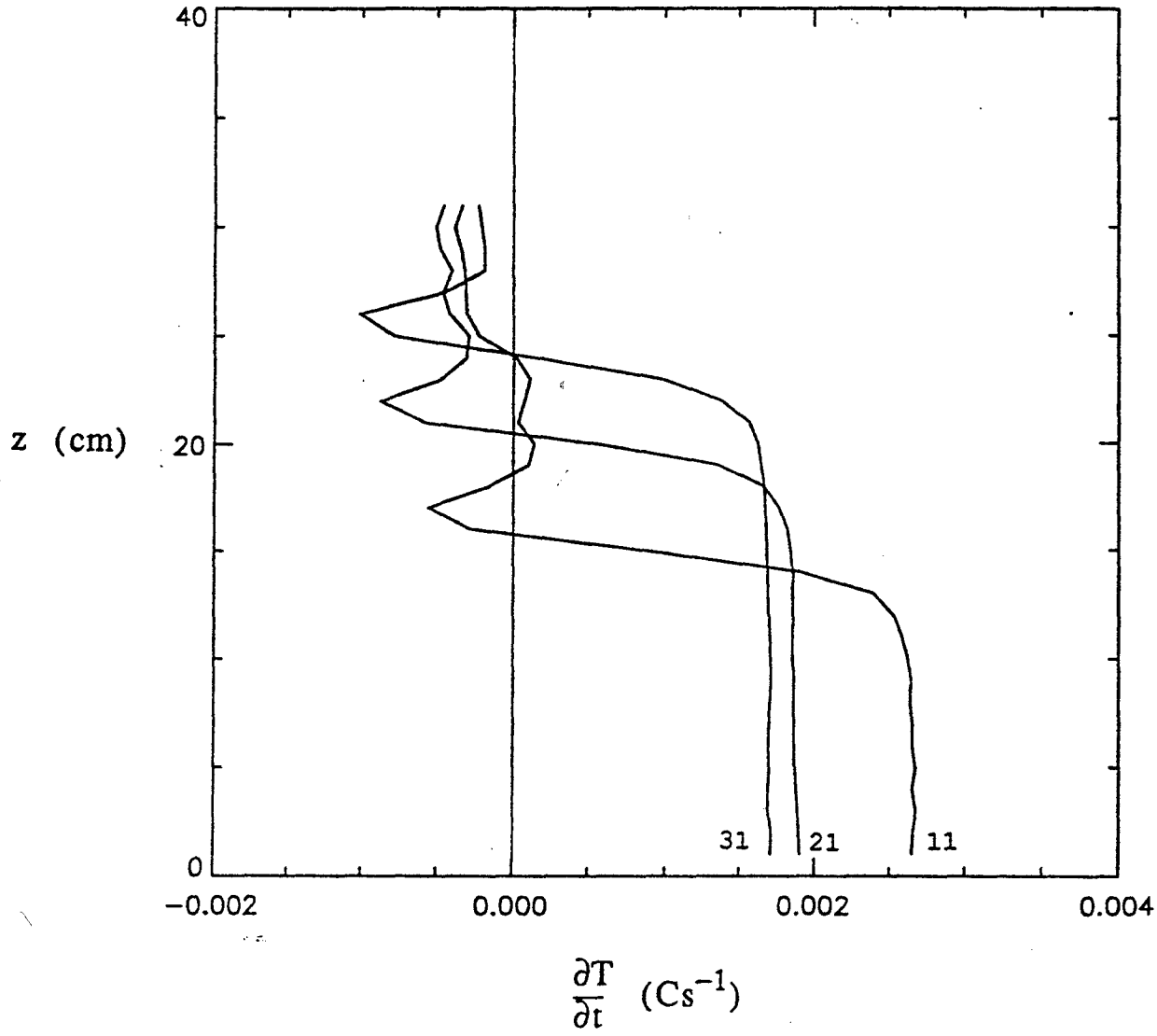

Figure 2. Time rate of change of mean temperature for three traverses.

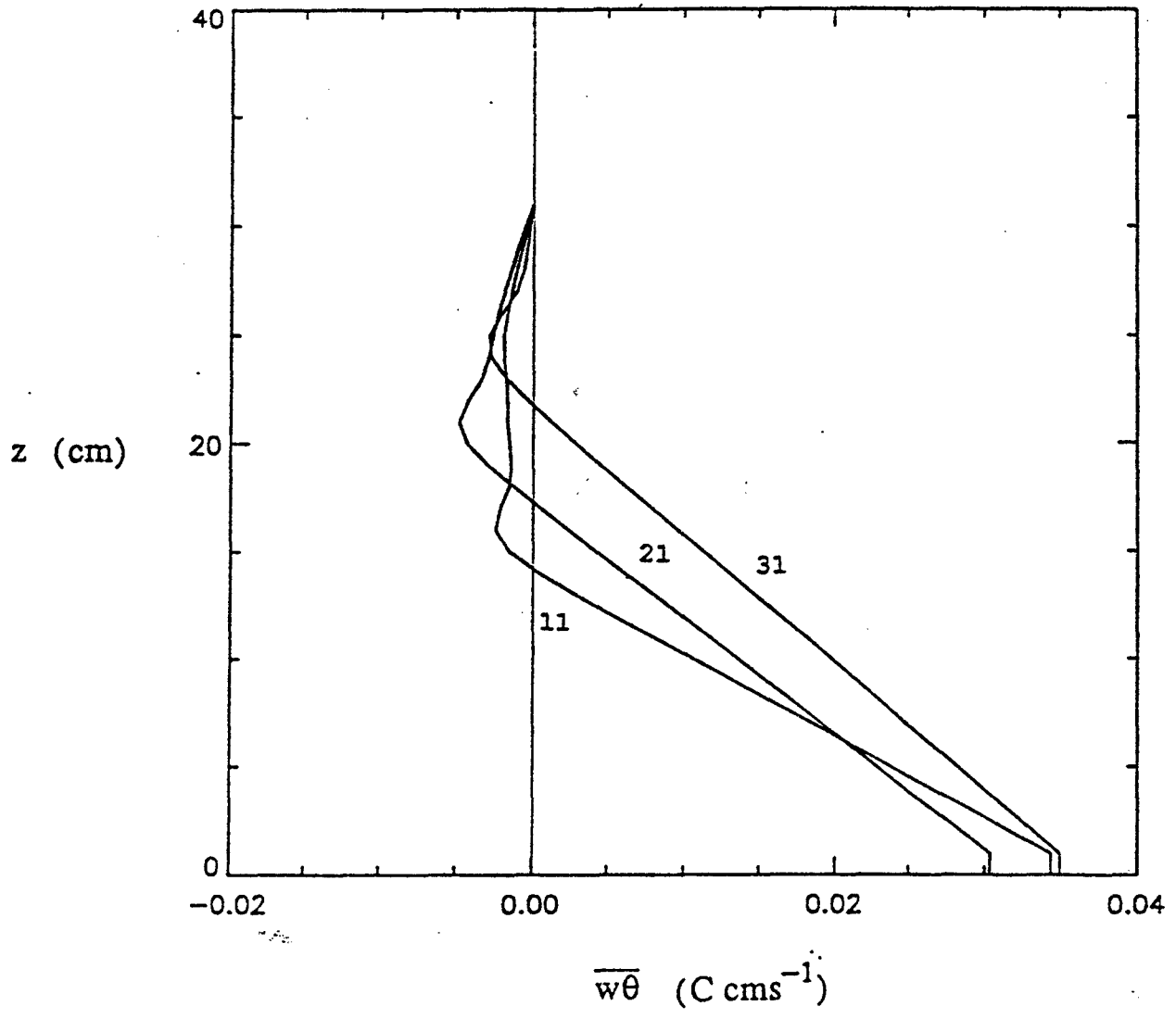

Figure 3. Deduced vertical temperature flux profiles for three traverses.

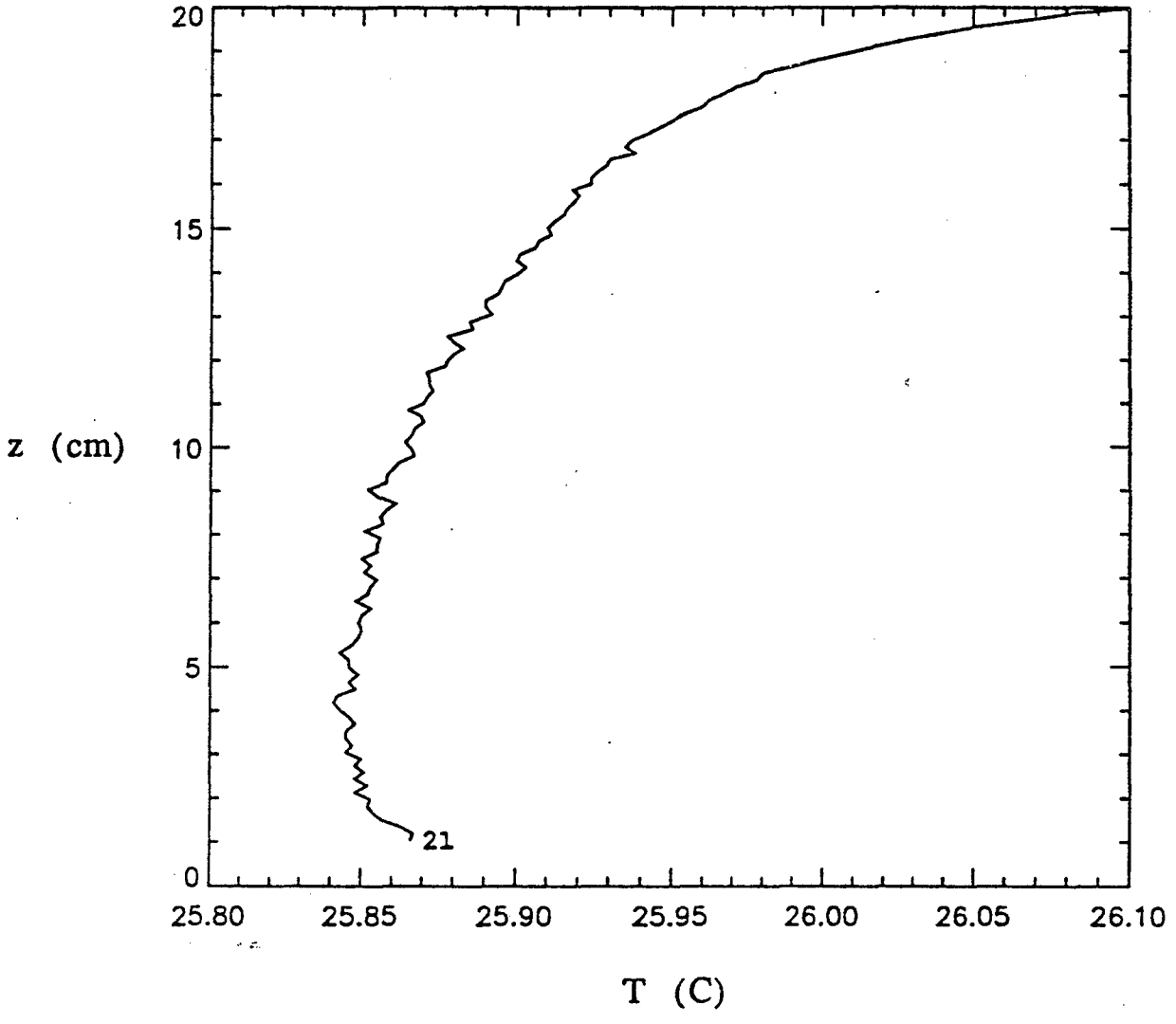

Figure 4. An expanded record of mean temperature versus height and time for traverse 21.

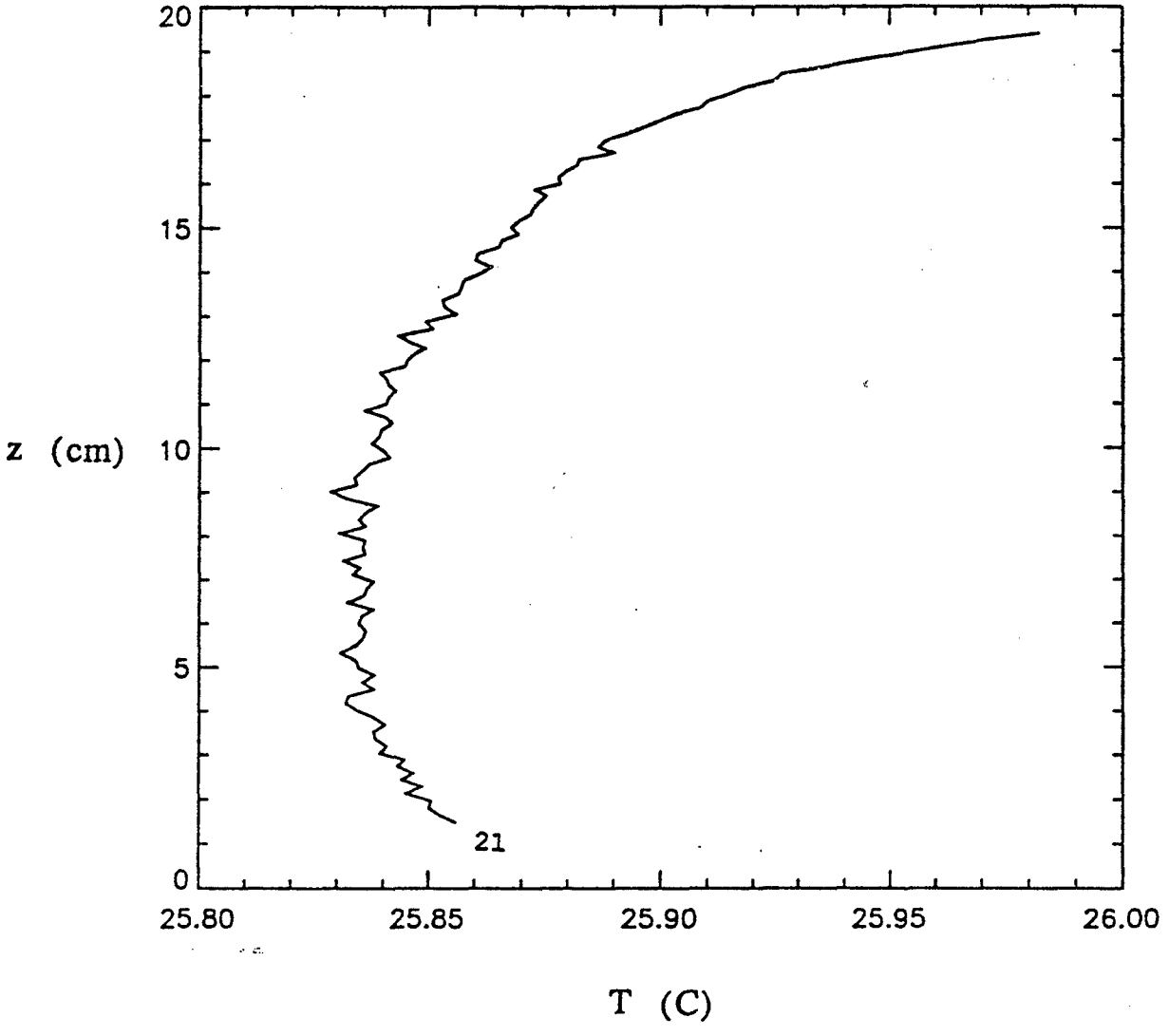

Figure 5. An expanded record of mean temperature versus height for traverse 21.

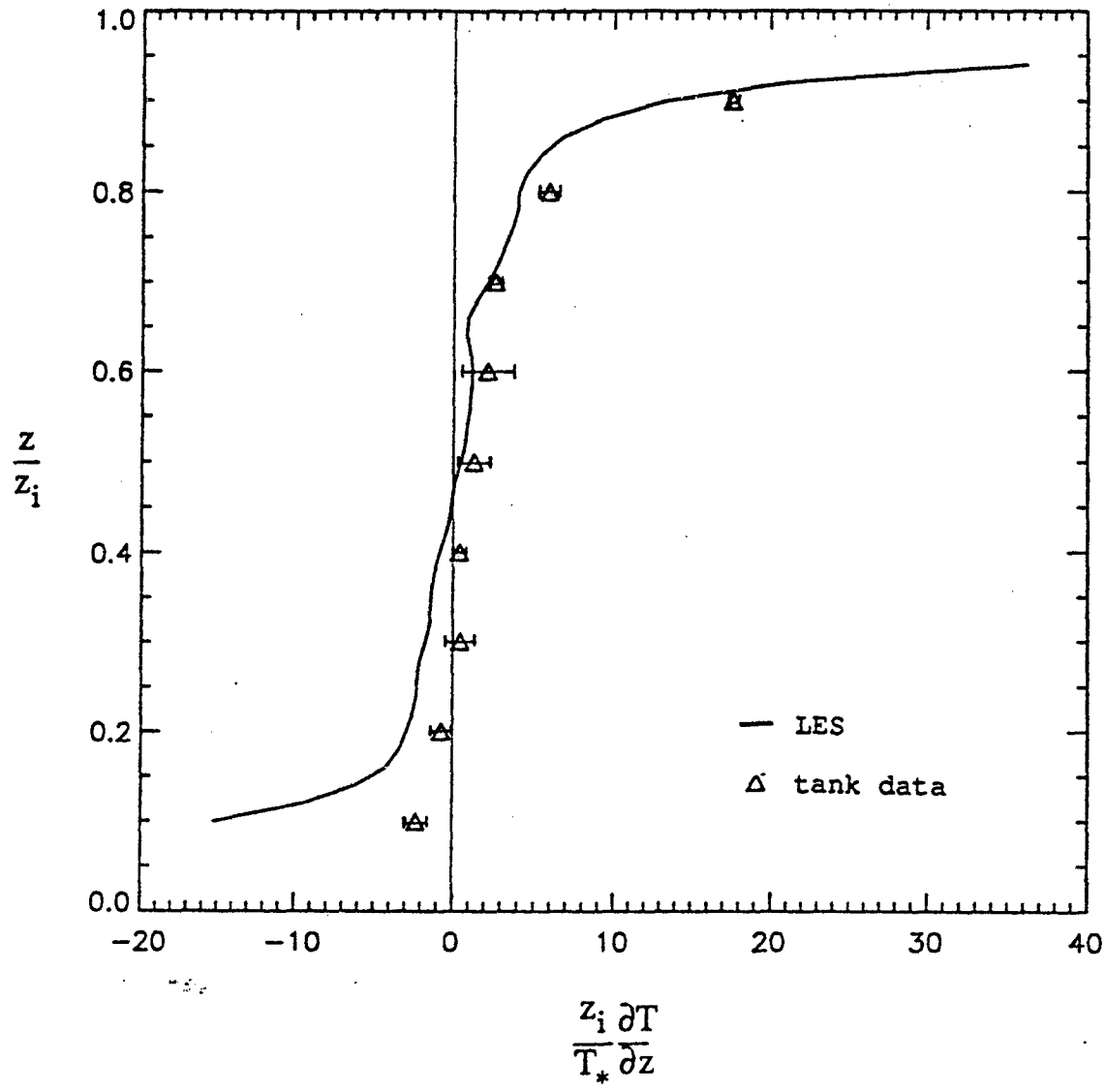

Figure 6. Nondimensionalized mean temperature gradient compared with LES results. The data points indicate the average over the three traverses; brackets indicate the standard deviation.

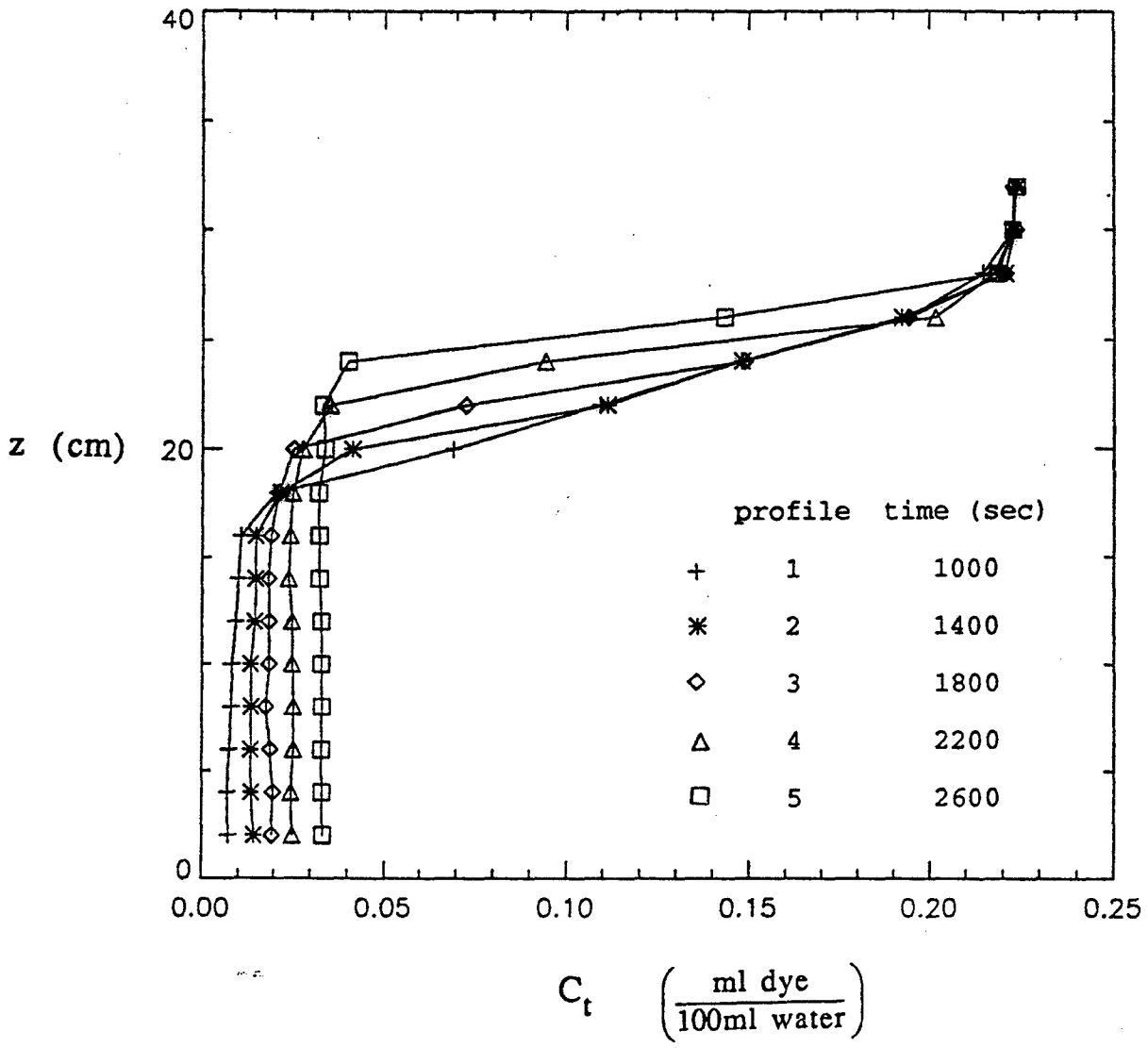

Figure 7. Mean dye concentration versus height at five times.

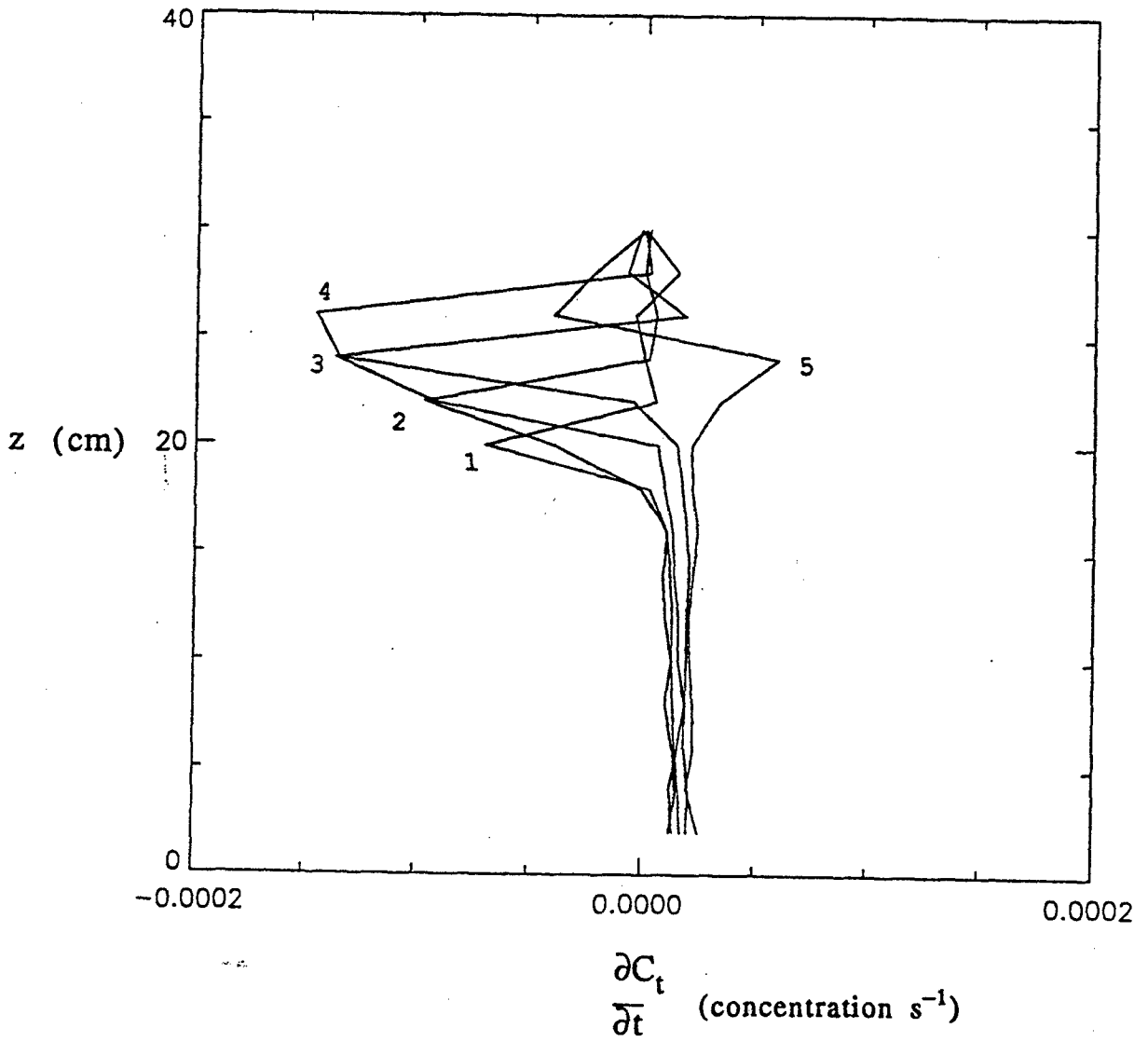

Figure 8. Time rate of change of mean dye concentration versus height at five times.

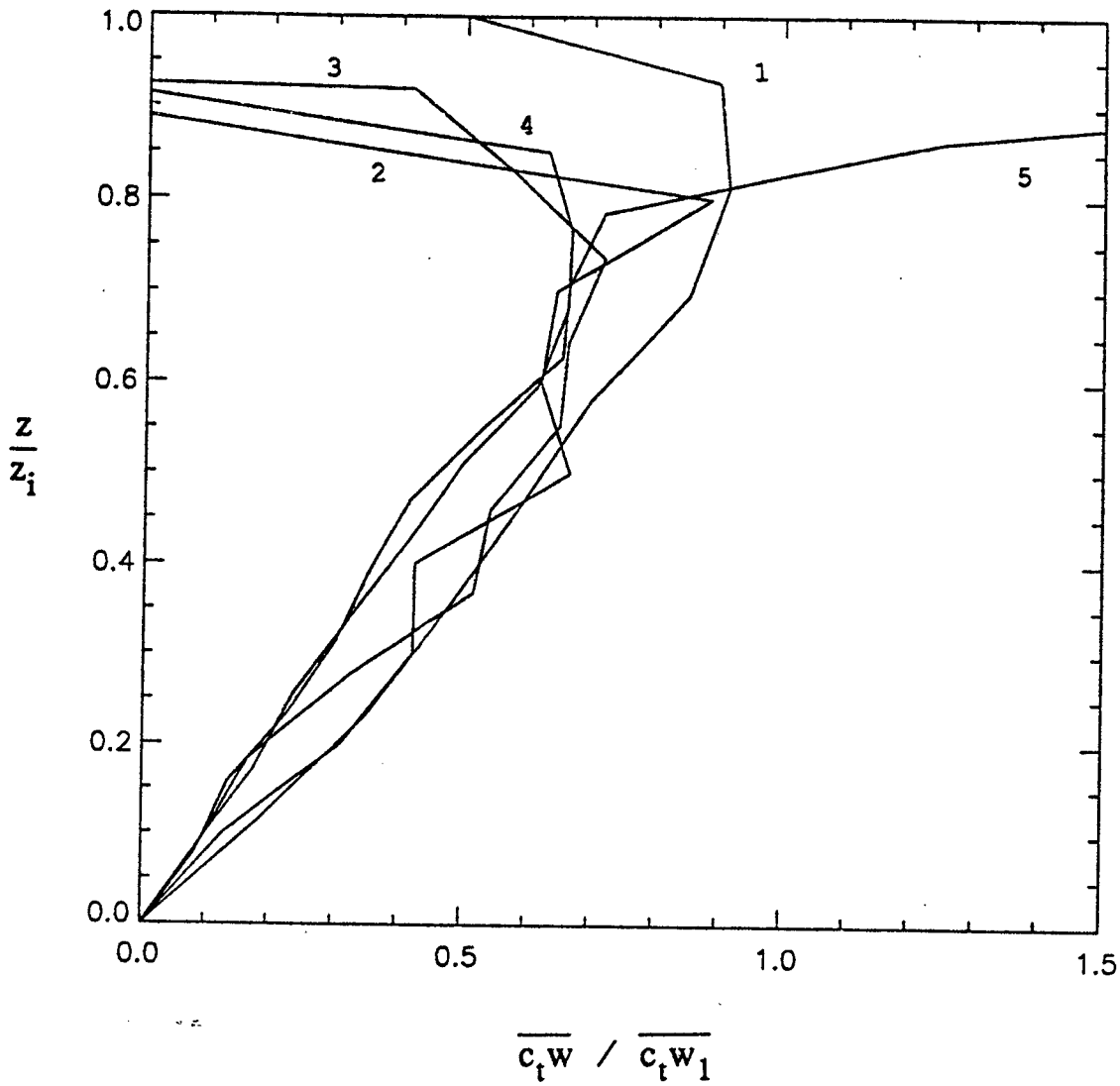

Figure 9. Deduced vertical concentration flux profiles at five times.

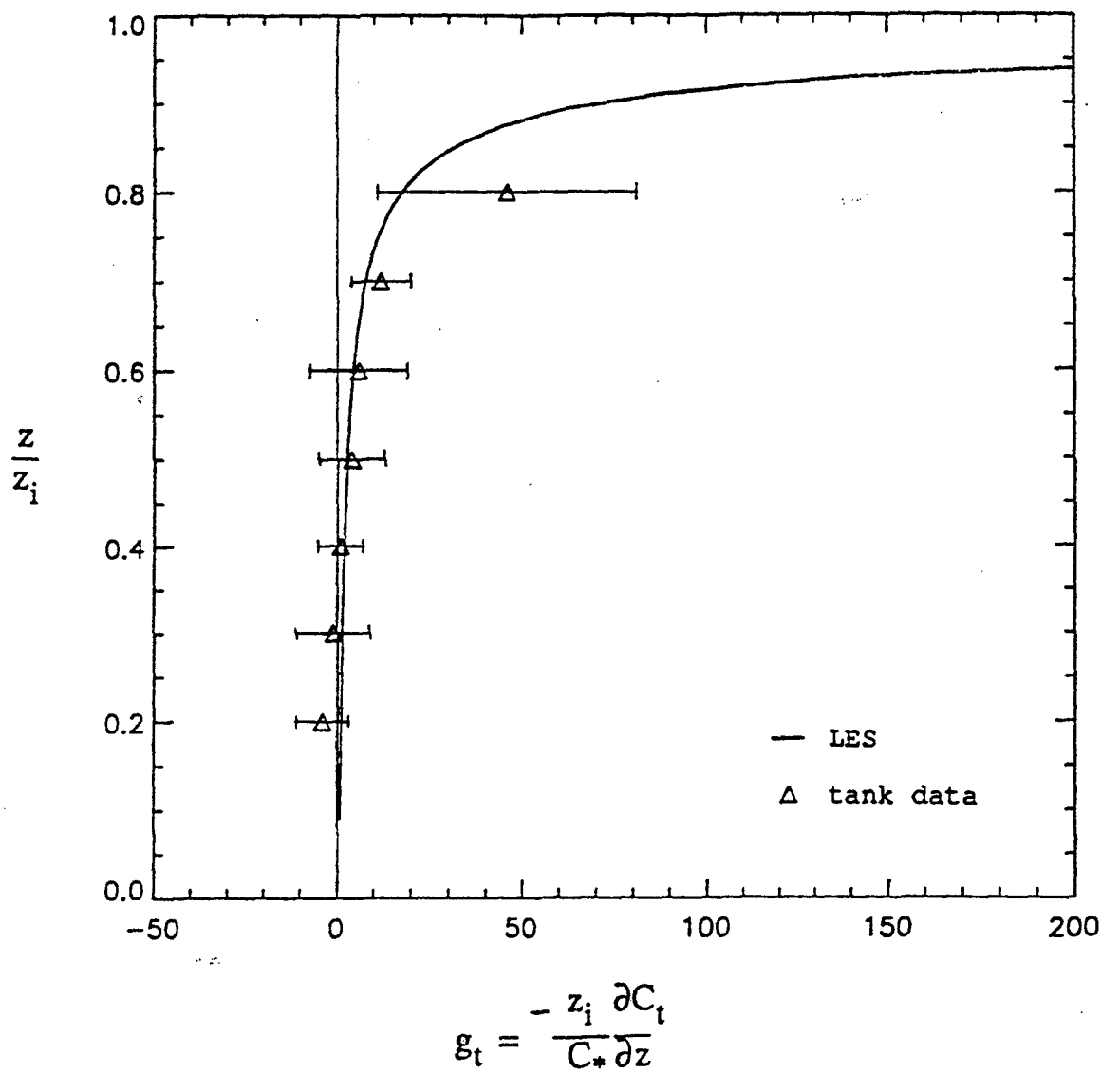

Figure 10. The dimensionless top-down gradient function g_t compared with LES results. The data points indicate the average over the five times; brackets indicate the standard deviation.

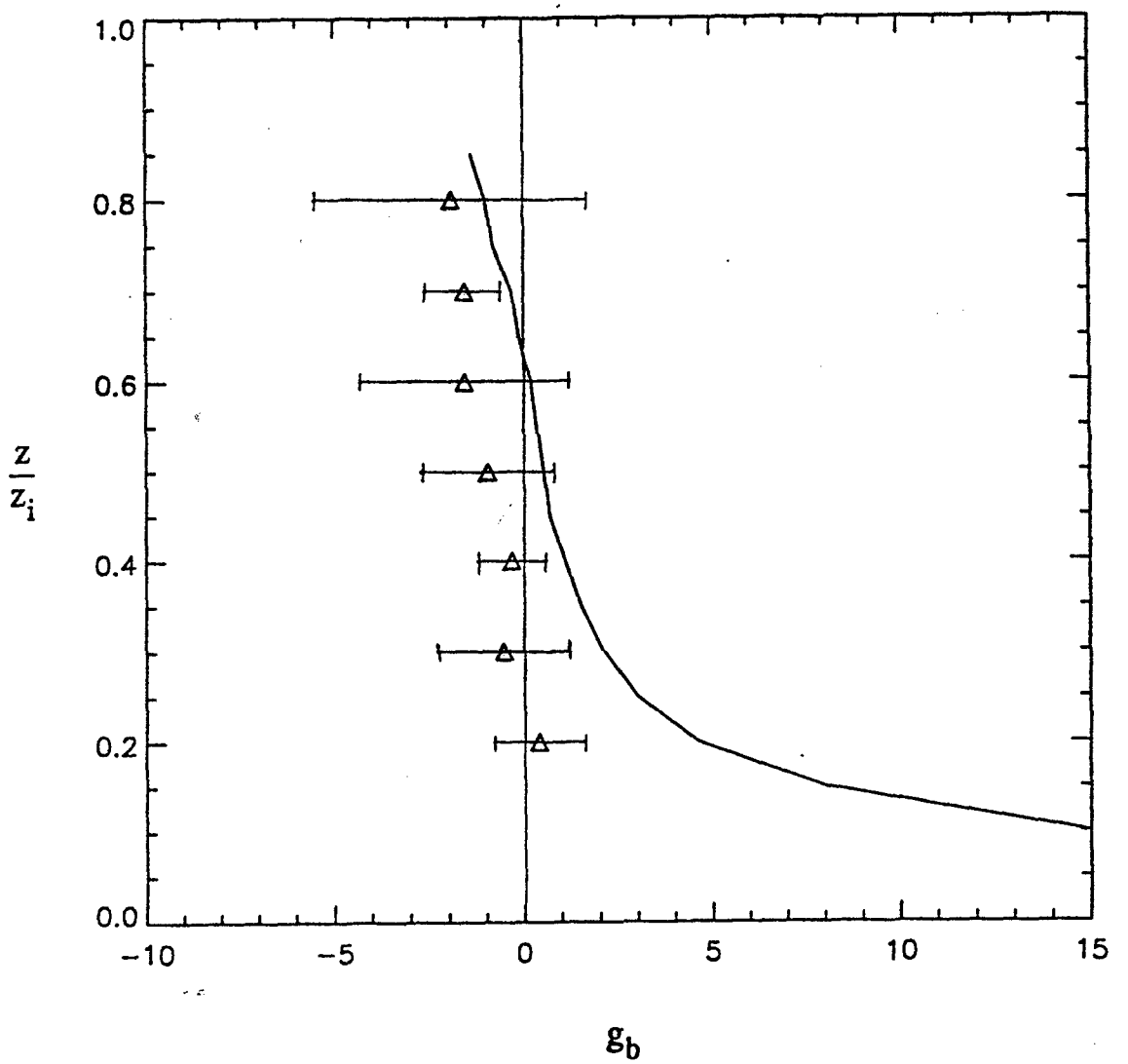

Figure 11. The deduced bottom-up gradient function g_b compared with the LES results. The data points indicate the average over the three traverses and five times; the brackets denote the standard deviation.